ISTITUTO NAZIONALE DI FISICA NUCLEARE

Laboratori Nazionali
di Legnaro

INFN/BE-82/4
1 Dicembre 1982

G. D'Erasmo, D. Fabris, F. Gramegna, I. Iori, A. Moroni, G. Nebbia, A. Pantaleo, G. Prete, R. A. Ricci, G. Viesti and Li Zu Yu: PROGRESS REPORT ON HEAVY ION IDENTIFICATION BY BRAGG CURVE SPECTROSCOPY AT THE LEGNARO XTU TANDEM LABORATORY

Servizio Documentazione
dei Laboratori Nazionali di Frascati

Istituto Nazionale di Fisica Nucleare
Laboratori Nazionali di Legnaro

INFN/BE-82/4
1 Dicembre 1982

G. D'Erasmo[x], D. Fabris, F. Gramegna, I. Iori[o], A. Moroni[o], G. Nebbia, A. Pantaleo[x], G. Prete, R. A. Ricci[+], G. Viesti[+] and Li Zu Yu[•]:

PROGRESS REPORT ON HEAVY ION IDENTIFICATION BY BRAGG CURVE SPECTROSCOPY AT THE LEGNARO XTU TANDEM LABORATORY

ABSTRACT

The experimental work on heavy ion identification by Bragg Curve Spectroscopy at the XTU Tandem Laboratory is summarized.

The problems in using BCS detectors and the lines of future work are discussed.

1. - INTRODUCTION

In the last years gas filled ionization chambers (I. C.) increased their importance for particle identification in heavy ion detection systems[1], often substituting the usual semiconductor ΔE-E telescopes.

In fact the gas detectors have better ΔE thickness uniformity, do not suffer radiation damage, have no pulse height defect and are capable to match any desired geometry.

Recently Gruhn et al.[2] proposed an alternative utilization of the I. C. in the detection of heavy ions: the Bragg Curve Spectroscopy (BCS). Experimental results obtained in different laboratories using the BCS technique have been already published[3, 4, 5].

(x) - INFN, Sezione di Bari, and Istituto di Fisica dell'Università di Bari.
(o) - INFN, Sezione di Milano, and Istituto di Fisica dell'Università di Milano.
(+) - and Istituto di Fisica dell'Università di Padova.
(•) - Institute of Modern Physics, Lanzhov, R. P. C.

The aim of this report is to summarize the experimental work done at the XTU Tandem accelerator of the Legnaro National Laboratories in this field.

The problems in using BCS detectors and the lines of future work will be also discussed.

2. - THE BRAGG CURVE SPECTROSCOPY

2. 1. - The BCS concept

It is known from early times[6] that the average specific ionization versus the range (the Bragg Curve) of a charged particle in a gaseous medium is characteristic of the ionizing particle. In fact the mean energy W necessary to form an ion pair is nearly independent of the particle velocity[7] so that the specific ionization along the track is proportional to the specific energy loss.

From the Bragg Curve the following quantities can be defined:

a) the total kinetic energy E as the integral of the specific ionization over the whole track;

b) the range R as the length of the track;

c) the energy loss ΔE as the specific ionization at the beginning of the track;

d) the Bragg Peak (BP) as the maximum of the specific ionization.

The BCS basic idea is to identify the heavy ions by measuring the above set of quantities, which characterize the slowing down process of the particles detected in the I. C. gaseous medium. Considering a particle of mass A, nuclear charge Z and velocity $\beta = v/c$, the following dependences hold:

$$E \cong E(A, \beta);$$

$$R = R(A, Z, \beta);$$

$$\Delta E = \Delta E(Z, \beta);$$

$$BP = BP(Z).$$

The BP amplitude determines unambiguously Z and is independent of the energy if the particle velocity is higher than that corresponding to the maximum stopping power in the Bragg Curve.

The BCS technique offers several advantages respect to the traditional ionization chamber:

a) The atomic number Z is identified by the BP amplitude and there is also redundancy in Z measurement (ΔE, R).

b) By combining BP, R and ΔE measurements, it is possible, in principle, to identify the mass of the detected ion.

c) High resolution are possible on the BCS parameters because all the measurements are made in one medium, eliminating window or dead layer effects.

While particle identification by ΔE-E or R-E measurements are popular using I. C., the detection of the Bragg Peak is typical of the BCS method.

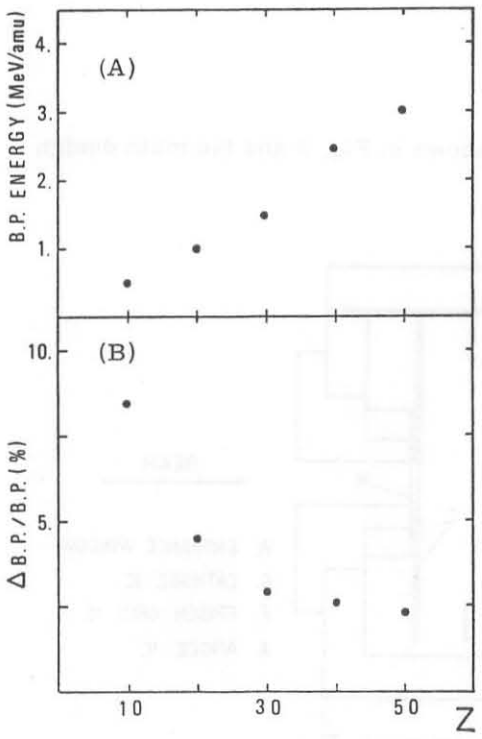

In Fig. 1 crude predictions are reported, using Argon as stopping medium[8, 9], on the specific energy (in MeV/amu) at which the BP occurs (part A) and on the percent BP amplitude difference between neighbouring atomic numbers (part B) as a function of Z. The predicted BP difference is $\Delta BP/BP > 2\%$ up to $Z = 50$. It should be also noticed that the BP energy depends on the atomic number of both the detected particle and the stopping medium so that the limit for the BP detection may be lowered using low Z counting gas.

FIG. 1 - Prediction on the specific energy at which the Bragg Peak occurs (A) and on the percent Bragg Peak amplitude difference between neighbouring elements (B) as a function of Z for heavy ions in Argon[8, 9].

2. 2. - BCS detector design

A BCS detector is an I. C. with the electric field parallel to the particle trajectories.

The Frish grid to cathode distance is longer than the range of the particles to be stopped and the anode to grid distance is shorter than the lowest range of interest. The particles enter the I. C. through the cathode and leave an ionization track parallel to the electric field. The electrons along the track are drifted through the grid and the time dependence of the current is a measure of the specific ionization along the track (Fig. 2).

In this way the grid to anode distance determines the sampling step of the Bragg curve.

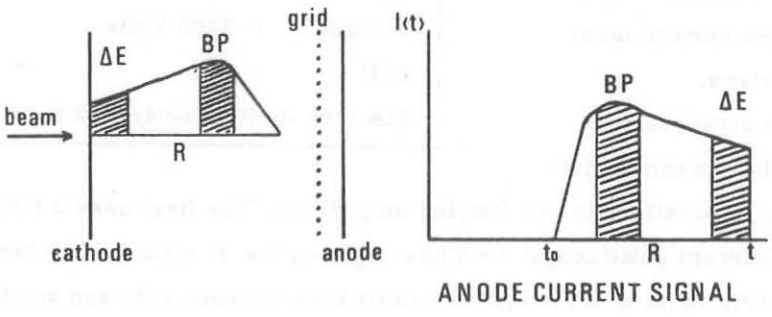

FIG. 2 - The Bragg Curve Spectroscopy concept.

3. - THE LEGNARO BCS IONIZATION CHAMBER

3.1. - Detector lay-out

A cross sectional view of the LNL BCS detector is shown in Fig. 3 and the main design parameters are reported in Table I.

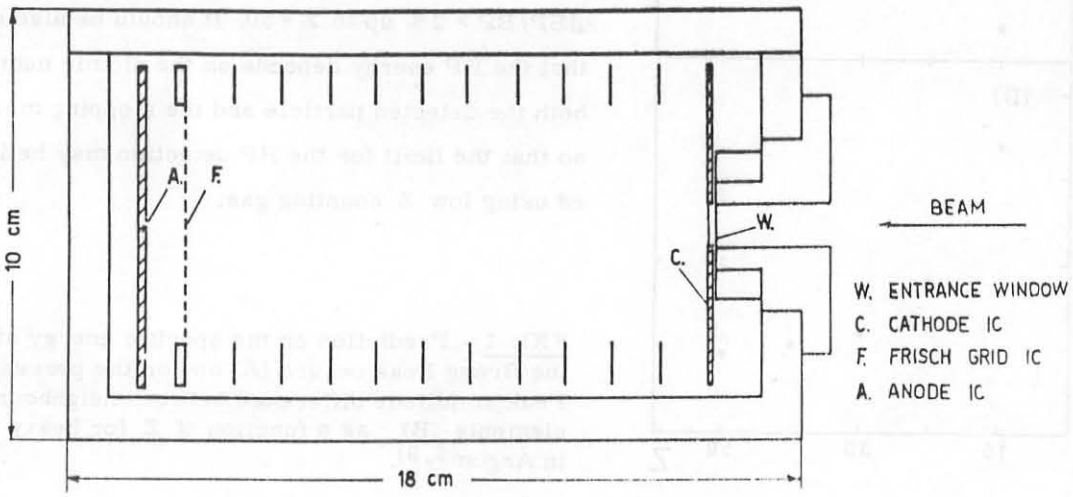

FIG. 3 - Cross sectional view of the BCS detector.

The voltage and pressure values reported have been used during the measurements reported below.

The voltage between the Frish grid and the cathode is divided by a resistor chain, connected to potential guard rings to obtain a homogeneous electric field over the whole detector volume. Conventional NIM electronics have been used to measure the BC parameters.

TABLE I - BCS-IC Desing Parameters

Cathode to grid distance	: 12 cm
Grid to anode distance	: 1 cm
Grid	: 20 line per inch copper mesh
Window	: 1.5 μm thick Mylar, 3 cm diameter
Gas	: high purity i-Butane p = 180 torr
V cathode	= 0 Volts
V grid	= 1900 Volts
V anode	= 2700 Volts
E/P	= 0.9
Electron drift velocity	= 2.5 cm/nsec

The I. C. anode signal is fed into a charge sensitive preamplifier which is connected, in parallel, to two shaping amplifiers. The first uses a time constant longer than the maximum current pulse lenght (~ 5 μsec) giving the E signal. The latter uses a time constant approximately equal to the electron transit time between grid and anode. In this way the output signal of this amplifier is representative of the Bragg Curve within the accuracy of

the physical sampling step. This shaping amplifier is followed be a peak stretcher yielding the BP amplitude. To measure Range and ΔE the Bragg Curve signal is sent to a delay line amplifier. After the delay line shaping two signal are obtained; a positive signal proportional to the ΔE.

The time difference between them is a measure of the Range. It is then possible, in a simple way, to measure the whole set of parameters characterizing the Bragg Curve of the detected particle.

Some problems could arise in signal handling because of the large time spread of the signals relative to the same event, depending on the particle range.

Furthermore the above signal handling is only one way to analyze the Bragg Curve and alternative systems are possible.

Fig. 4 shows an example of the results obtained with the BCS method in the case of 150 MeV ^{32}S ions elastically scattered by a Au target at $\theta_{LAB} = 40^{o}$. Beyond the elastic peak, slit scattered particles show the evolution of the BP, ΔE, R parameters as a function of the detected energy. The arrows mark the energy for R = = 1 cm (grid to anode distance). For lower energies the particle track is R < 1 cm so that there is no sampling of the Bragg Curve and the two shaping amplifiers handle the same amount of ionization charge. Therefore BP and ΔE are approximately proportional to E. For higher energies (R > 1 cm) the BP and ΔE behaviour (ionization at the end and at the beginning of the track) becomes different: BP remains constant with the energy, while ΔE decreases following the dE/dx vs E dependence.

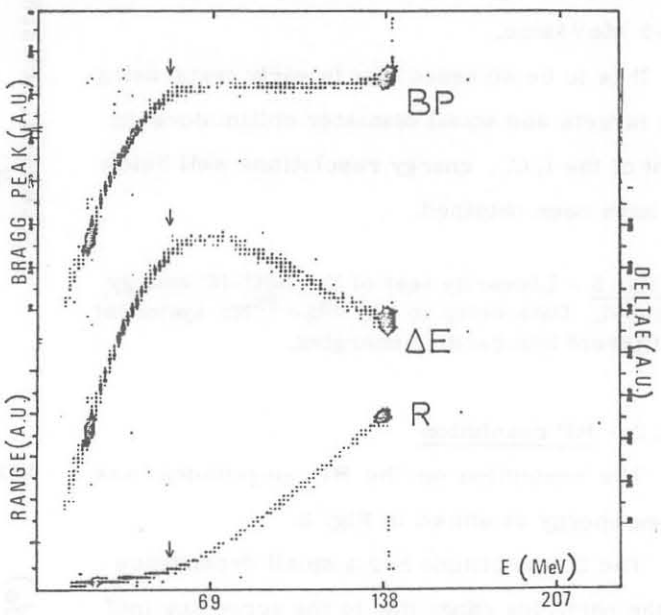

FIG. 4 - BP, ΔE, R vs E scatter plots for $^{32}S + ^{197}Au$ at E = 150 MeV and $\theta_{LAB} = 40^{o}$. The arrows mark the energy for R = 1 cm.

3. 2. - Experimental resolutions

At the beginning of 1982 the XTU Tandem beams allowed tests to experimental devices and measurements of heavy-ion induced reactions. The BCS-IC, after short test runs to check the detector capability, was employed in studying ^{32}S and ^{28}Si induced reactions at ~ 5 MeV/amu on various targets, ranging from ^{27}Al to ^{100}Mo. The experimental data

reported below are overall resolutions (fwhm) measured on the "elastic" peak during the reaction studies. Typically target thicknesses were 100-200 $\mu g/cm^2$ and the detector was positioned 40 cm from the target at laboratory angles ranging from 6^o to 55^o viewing $\Delta\theta = 0.9^o - 1.5^o$ in the reaction plane. With this geometry the time needed to collect spectra with enough statistic was 1-12 hours depending on the reaction and on the observation angle.

3. 2. 1. - Energy resolution

The measured energy resolution was $\delta E/E$ = 1-1.5 %. Calibration's runs at different ^{32}S beam energies demonstrated the good energy linearity of the detector (as shown in Fig. 5) and a constant energy resolution in the energy range 2.6-5 MeV/amu.

It is to be stressed that in early tests using thin targets and small diameter collimators in front of the I. C., energy resolutions well below 1 % have been obtained.

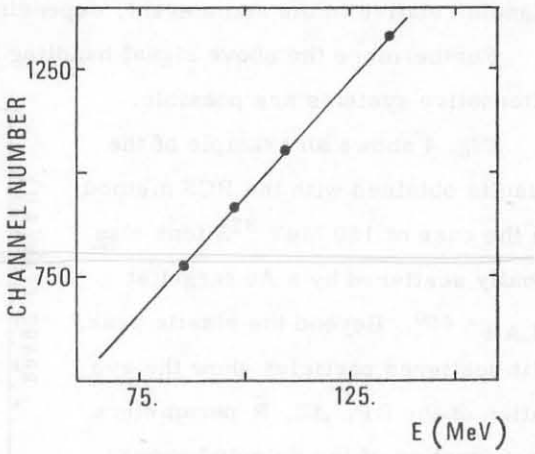

FIG. 5 - Linearity test of the BSC-IC energy signal. Data refer to the $^{32}S + ^{93}Nb$ system at different bombarding energies.

3. 2. 2. - BP resolution

The resolution on the BP amplitudes was $\delta BP/BP$ = 1.7-2 % independent of the particles energy as shown in Fig. 6.

The BP amplitude has a small dependence on the particles range due to the screening inefficiency of the Frisch Grid. Because of this inefficiency the charge produced near the grid induces a signal on the anode just before to be drifted through the grid. This effect can be corrected in the off-line data analysis.

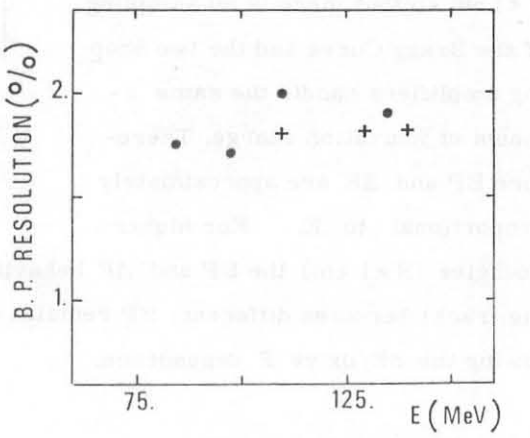

FIG. 6 - BP resolution vs energy for the $^{32}S + ^{93}Nb$ (•) and $^{32}S + ^{100}Mo$ (+) systems at different bombarding energies.

3. 2. 3. - Range and E resolutions

The range resolution was $\delta R/R$ = 2.1-3.1 % depending on the ion energy as shown in Fig. 7. This range resolution corresponds to a time resolution $\delta t \approx 100$ nsec (fwhm) obtained

using the positive and negative signals after the delay line shaping.

The resolution on the ΔE amplitude (negative portion of the delay line output signal) was $\delta\Delta E/\Delta E = 2.7\text{-}3.7\%$ depending on the ion energy. This resolution is quite similar to that obtained with classical ΔE gaseous counters in the same range of projectiles and energies[10].

These resolutions depend on the experimental conditions and on the signal handling so that better results could be obtained.

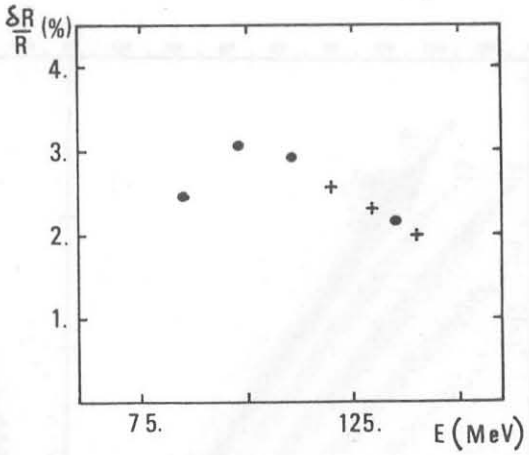

FIG. 7 - R resolution vs energy for the $^{32}S + ^{93}Nb$ (•) and $^{32}S + ^{100}Mo$ (+) systems at different bombarding energies.

4. - ELEMENTAL RESOLUTION

In this section we report on the identification of the elements produced in nuclear reactions induced by heavy ions using the BCS-IC.

Figs. 8 show scatter plots of BP vs E, R vs E, ΔE vs E as they appear at the computer screen in the off-line data replay. Data refer to the ^{32}S on ^{100}Mo reaction at 150 MeV bombarding energy and $\theta_{LAB} = 35^{o}$.

The BP vs E scatter (Fig. 8a) shows a good separation of the various elements ($Z = 12\text{-}15$) produced in the nucleus-nucleus collisions. As can be seen the BP amplitude is constant with the energy in the range of interest showing deviations at the higher and lower energies due to the effects discussed in the previous section.

A clear separation between the elements is present also in the R vs E (Fig. 8b) and ΔE vs E (Fig. 8c) scatter plots showing the power of the BCS method in the element identification.

The comparison of BP and ΔE (or R) vs E scatter plots is also indicative of the advantages in handling energy independent signals, as the BP, instead of energy dependent ones, as ΔE (or R), to obtain fast charge gates.

Fig. 9 shows the projection on the BP axis of the scatter plot of Fig. 8a ($65 \lesssim E \lesssim 140$ MeV) after a range dependent correction to account for the grid screening inefficiency. The measured Z resolving power is $Z/\Delta Z \sim 45$ at $Z = 16$ for the energy integrated spectrum. Similar results on the Z-resolving power have been obtained in the case of the $^{32}S + ^{27}Al$ data[5].

The linearity of the BP amplitude has been checked as follows.

In Fig. 9 the arrows mark the predicted position on the BP axis of the elements $Z = 8$ to 20 using calculated data[11] of H. I. stopping power in isobutane normalized at $Z = 16$ and $Z = 11$ to the experimental data. The agreement in the Z-position between experimental and cal

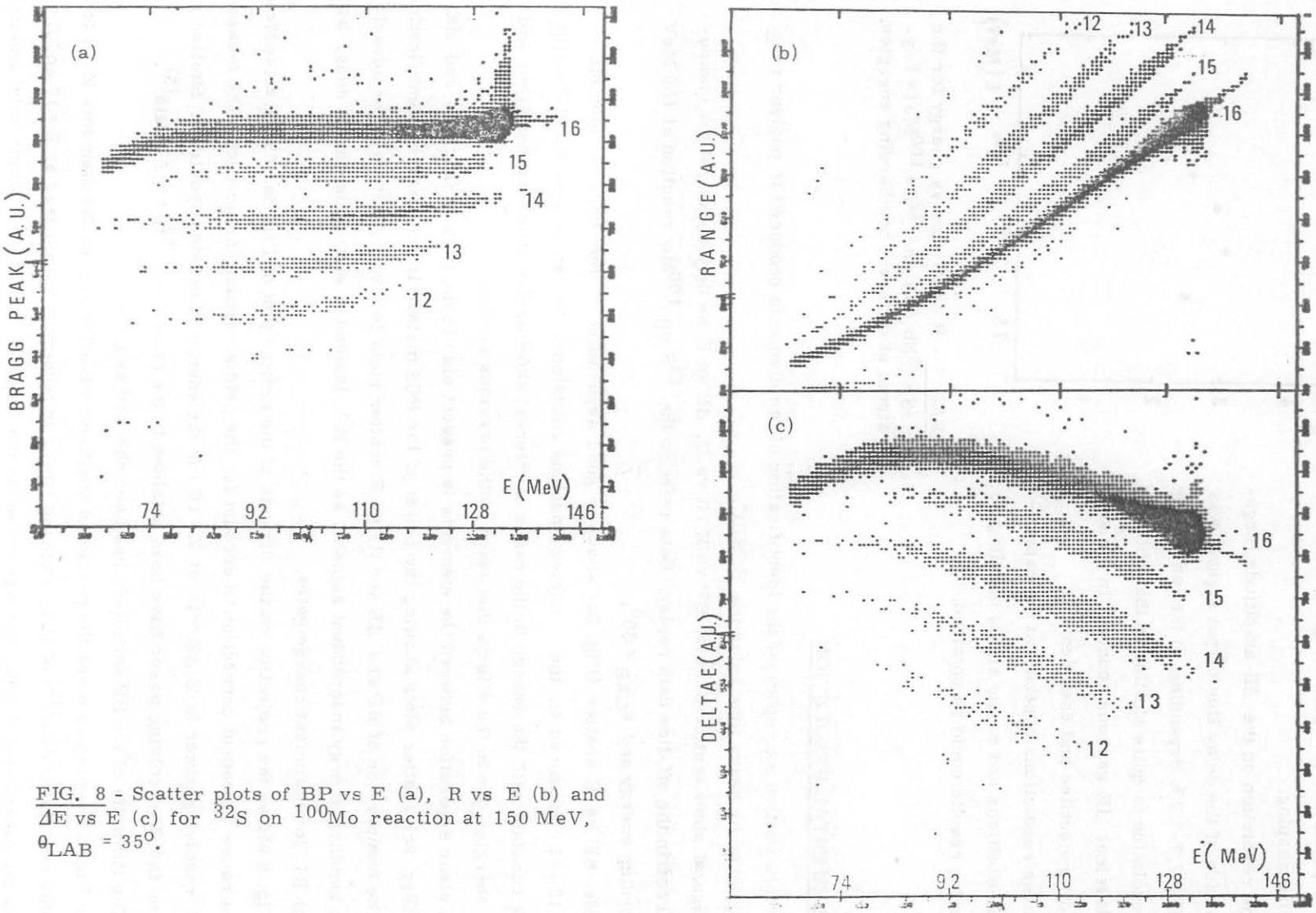

FIG. 8 - Scatter plots of BP vs E (a), R vs E (b) and ΔE vs E (c) for ^{32}S on ^{100}Mo reaction at 150 MeV, $\theta_{LAB} = 35^{o}$.

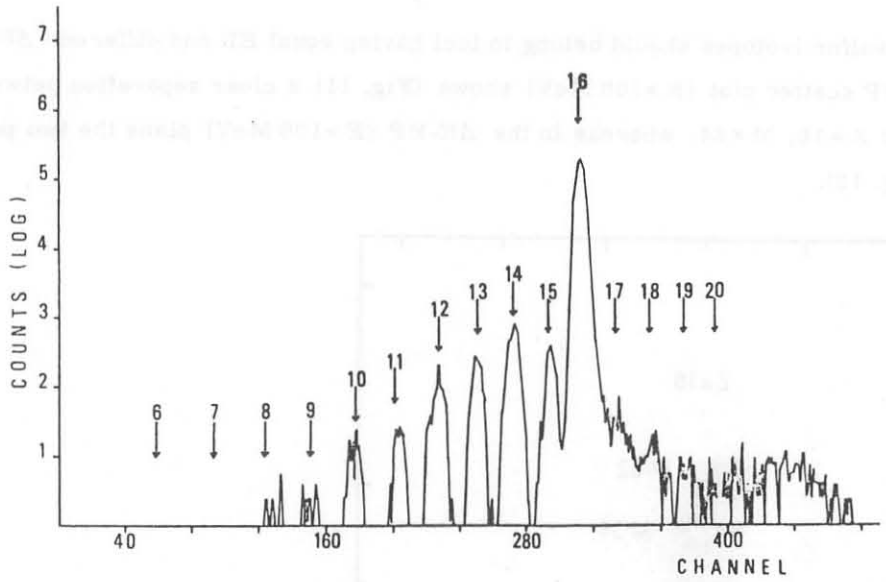

FIG. 9 - Projection of the BP axis of the scatter plot in Fig. 8a after a small range dependence correction. The Z-resolving power is $Z/\Delta Z \sim 45$ at $Z = 16$. The arrows mark the predicted position on the BP axis of the elements $Z = 8$ to 20.

culated value is very good and it extends well far from the normalization points.

Using the calculated stopping power normalized to the experiments, it is possible to predict the achievable Z-resolving power by B. P. detection in i-butane. Fig. 10 shows the predicted power in the case of resolution on the BP amplitude $\delta BP/BP = 1$ and 2%. As can be seen with the 2% resolution, elements up to $Z \sim 40$ could be identified, while a 1% resolution leads to the identification up to $Z \sim 80$. Obviously this results may be improved adding to the BP the ΔE and R information[2].

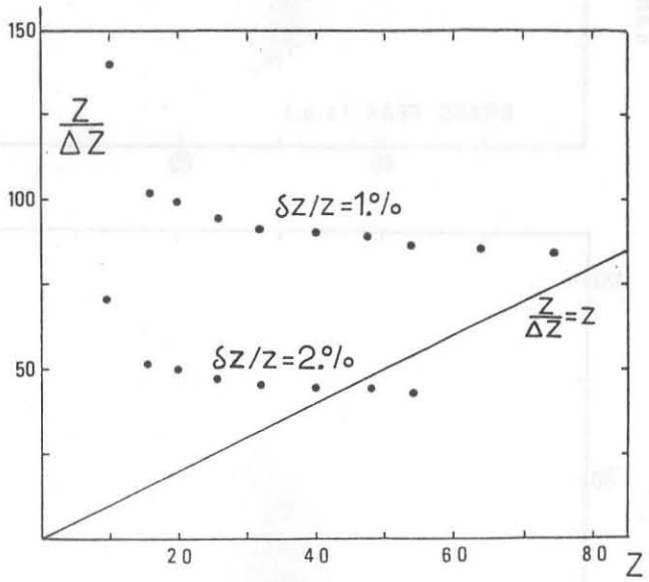

FIG. 10 - Predicted Z-resolving power of heavy ions in i-butane for BP amplitude resolutions $BP/BP = 1$ and 2%.

5. - MASS SENSITIVITY OF BC PARAMETERS

The mass sensitivity of BC parameters was studied detecting 150 MeV ^{32}S and ^{34}S ions elastically scattered by a ^{100}Mo target at $\theta_{LAB} = 35^{\circ}$. Since it holds $\Delta E = \Delta E(Z, v)$ and R =

= R(A, Z, v) the sulfur isotopes should belong to loci having equal BP and different ΔE and R.

The R vs BP scatter plot (E >100 MeV) shows (Fig. 11) a clear separation between Z = = 16, M = 32 and Z = 16, M = 34, whereas in the ΔE-BP (E >100 MeV) plane the two peaks are overlapped (Fig. 12).

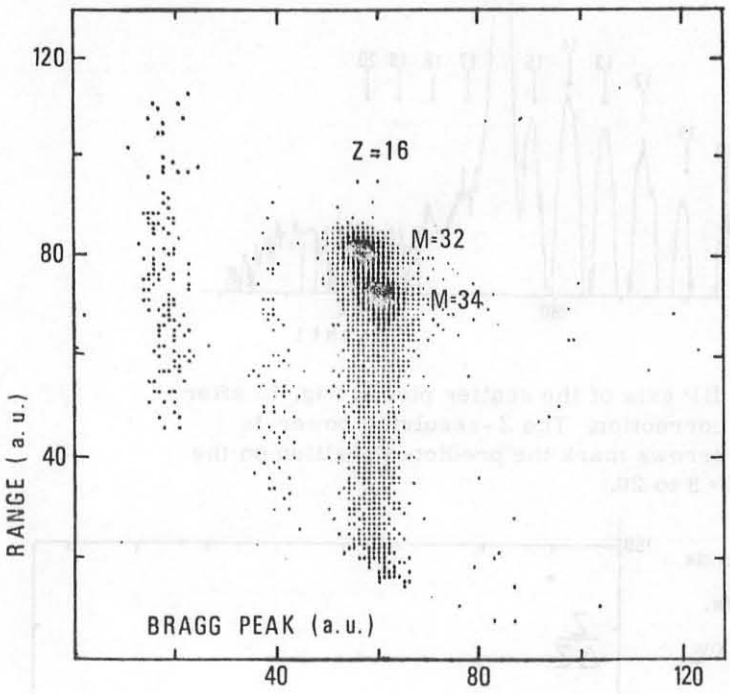

FIG. 11 - R vs BP plot for ^{32}S and ^{34}S ions elastically scattered by a ^{100}Mo target at $\theta_{LAB} = 35^{\circ}$ (E >100 MeV).

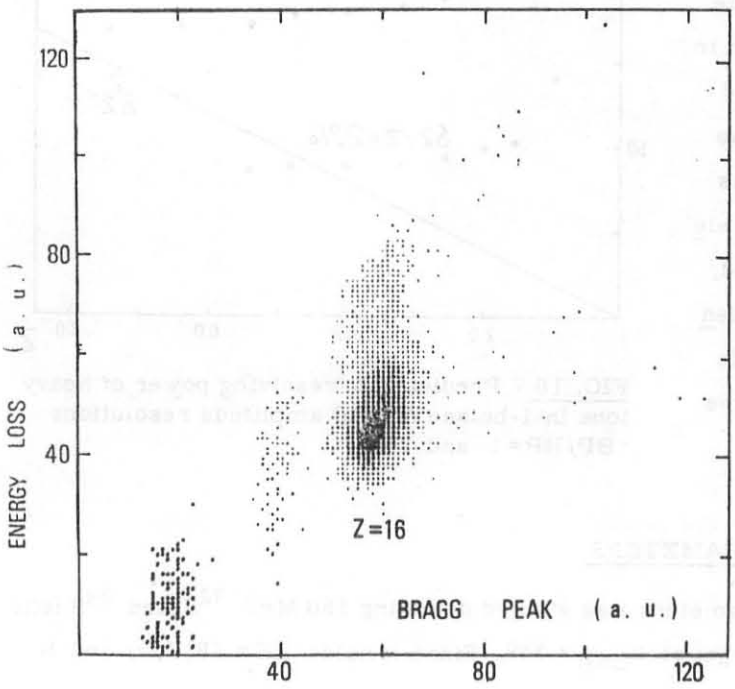

FIG. 12 - ΔE vs BP plot for the reaction as in Fig. 11.

It has to be noticed that also the BP shows a small mass dependence. It is due to the different charge distributions along the particle track: that induce a slightly different anode signal because of the grid screening inefficiency.

Evaluating the mass resolving power from the scatter plots some care has to be taken because of the different total energy released by the S isotopes in the I. C. due to the small kinematic effects and to the energy loss difference in the entrance window.

In a limited energy range, R is proportional to the kinetic energy E, so that the quantity E/R should be a simple function of Z and M.

In Fig. 13 the E/R vs BP scatter plot is reported and Fig. 14 shows the projection on the E/R axis. The estimated mass resolving power is $M/\Delta M = 26$ at $M = 32$. The same result has been obtained looking at the R difference at fixed E in a R vs E plot.

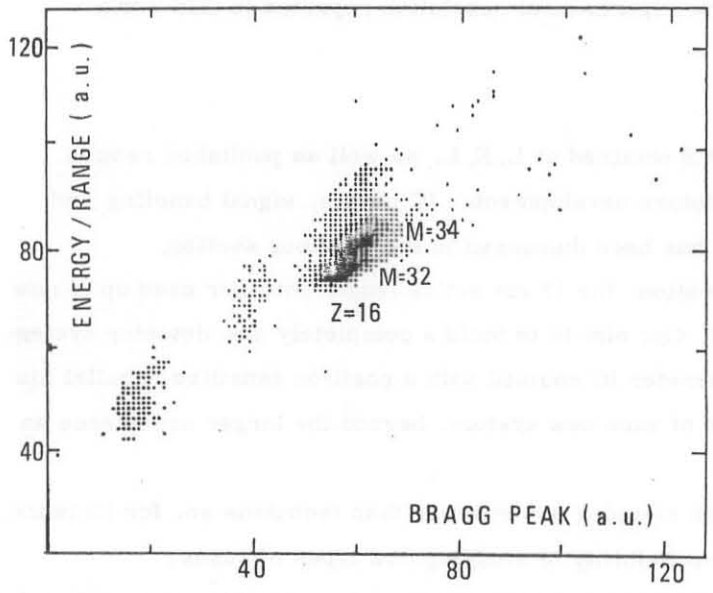

FIG. 13 - E/R vs BP plot for the reaction as in Fig. 11.

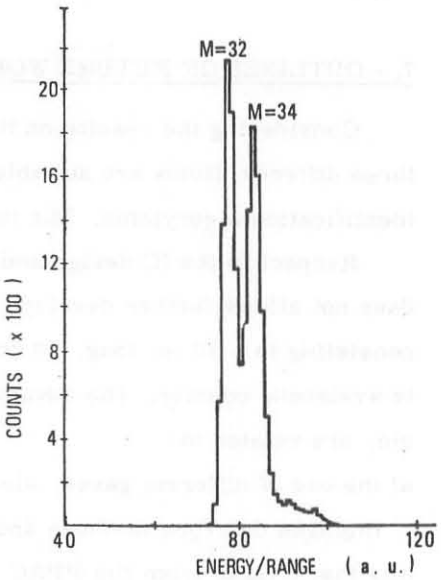

FIG. 14 - Projection on the E/R axis of the scatter plot in Fig. 13. The estimated mass resolving power is $M/\Delta M = 26$ at $M = 32$.

This is only a first attempt to handle the BC parameter for mass identification and also in this case the power of the method has not been fully used.

6. - DISCUSSION OF THE EXPERIMENTAL RESULTS

The need to start the nuclear physics experimental program with heavy ion beams as soon as the operation of the 16 MV XTU Tandem facility started at L. N. L., forced us to use the BCS-IC before fully exploiting its powerful identification methods. Nevertheless good

results have been obtained and it is now possible to perform an accurate estimate of the achievable resolving powers.

We stress that, to our knowledge, the reported data are the first example of complete measurement of the BCS parameters and mass sensitivity.

Our present interest is in ^{32}S and ^{28}Si beams, so the elemental resolution obtained by BP measurement only is good enough and we neglect, at the moment, the elemental information arising from ΔE and R measurements.

The mass resolution, still obtained in a naive way, indicates that the method is highly promising. From this point of view the main problem is related to the use of suitable identification algorythm for complete identification of heavy ions using the BCS parameters.

The identification power of the BCS detector is certainly higher than that of conventional ΔE-E gas detector, even within the experimental resolution reported in this work.

7. - OUTLINES OF FUTURE WORK

Considering the results on the BCS obtained at L. N. L. as well as published results, three different fields are suitable to future developments: IC design, signal handling and identification algorythms. The latter has been discussed in the previous section.

Respect to the IC design and operation, the 12 cm active length chamber used up to now does not allows further developments. Our aim is to build a completely new detector system consisting in a 50 cm long, 20 cm diameter IC coupled with a position sensitive parallel plate avalanche counter. The advantages of such new system, beyond the larger acceptance angle, are related to:

a) the use of different gases, also with stopping power lower than isobutane as, for instance, methane or argon methane and the possibility of studying new types of gases;
b) a fast trigger from the PPAC for the range measurement and for coincidence experiments;
c) the use of a double Frish Grid to avoid unlinearity in the BP amplitude.

The fast trigger signal from PPAC should improve the range measurement also simplifying the signal handling. The measure of the specific ionizations between the beginning of the track (ΔE) and the BP using a multi-stretcher system should also give further possibility to optimize the Z and A identification.

We express our hearthly thanks to the "Tandem Group" who has provided the Tandem facility at the L. N. L. and to the Accelerator staff and technical services of the Laboratories for their continuous helpful support.

We wish to thank M. Morando for the help to use the Tandem on-line acquisition system and computing facility and G. Fortuna for several stimulating discussions about gas detectors.

Thanks are due to C. R. Gruhn (L. B. L., Berkeley) who sent us unpublished data and technical news on the Berkeley detector.

REFERENCES

(1) - H. Stelzer, Nuclear Phys. A354, 433 (1981).

(2) - C. R. Gruhn, M. Binimi, R. Legrain, W. Pang, M. Roach, D. K. Scott, A. Shotter, T. J. Symon, J. Wonters, M. Zisman, R. De Vries, Y. C. Peng and W. Sondheim, Nuclear Instr. and Meth. 196, 33 (1982).

(3) - Ch. Schiessl, W. Wagner, K. Hartel, P. Kienle, H. J. Körner, W. Mayer and K. E. Rehm, Nuclear Instr. and Meth. 192, 291 (1982).

(4) - H. Ikezol, Y. Tomita,, N. Shikazono and T. Murakami, Nuclear Instr. and Meth. 196, 215 (1982).

(5) - D. Fabris, F. Gramegna, G. Nebbia, G. Prete, R. A. Ricci, G. Viesti, I. Iori and A. Moroni, Lett. Nuovo Cimento 34, 115 (1982).

(6) - W. H. Bragg, Studies in Radioactivity (MacMillan and Co., 1912).

(7) - G. Kuop and W. Paul, in "Alpha, Beta and Gamma Ray Spectroscopy", ed. by K. Siegbahn (North-Holland, 1968), p. 32.

(8) - L. C. Northcliffe and R. F. Schilling, Nuclear Data Tables A7, 233 (1970).

(9) - H. H. Andersen and J. F. Ziegler, The Stopping and Range of Ions in Matter (Pergamon Press, 1977).

(10) - J. C. Adloff, D. Disdier, V. Rauch and F. Scheigling, CRN Rapport d'Activité 1979 (CRN 80-81, Strasbourg, 1980), p. 61.

(11) - P. Boccaccio and G. Viesti, Report INFN/BE-81/1 (1981).